





Article

Shaping 1,2,4-Triazolium Fluorinated Ionic Liquid Crystals

Carla Rizzo , Ignazio Fiduccia, Silvestre Buscemi, Antonio Palumbo Piccionello , Andrea Pace 
and Ivana Pibiri * Department of Biological, Chemical and Pharmaceutical Sciences and Technologies (STEBICEF),
University of Palermo, Viale delle Scienze, Ed. 17, 90128 Palermo, Italy

* Correspondence: ivana.pibiri@unipa.it; Tel.: +39-091-2389-7545

Abstract: The synthesis and thermotropic behaviour of some di-alkyloxy-phenyl-1,2,4-triazolium trifluoromethane-sulfonate salts bearing a seven-carbon atom perfluoroalkyl chain on the cation is herein described. The fluorinated salts presenting a 1,2,4-triazole as a core and differing in the length of two alkyloxy chains on the phenyl ring demonstrated a typical liquid crystalline behaviour. The mesomorphic properties of this set of salts were studied by differential scanning calorimetry and polarized optical microscopy. The thermotropic properties are discussed on the grounds of the tuneable structures of the salts. The results showed the existence of a monotropic, columnar, liquid crystalline phase for the salts tested. An increase in the temperature mesophase range and the presence of two enantiotropic mesophases for the sixteen-atom alkyloxy chain salt can be observed by increasing the length of the alkyloxy chain on the phenyl ring.

Keywords: ionic liquids; liquid crystals; fluorinated salts; heterocyclic; mesogens



Citation: Rizzo, C.; Fiduccia, I.; Buscemi, S.; Palumbo Piccionello, A.; Pace, A.; Pibiri, I. Shaping 1,2,4-Triazolium Fluorinated Ionic Liquid Crystals. *Appl. Sci.* **2023**, *13*, 2947. <https://doi.org/10.3390/app13052947>

Academic Editor: Yuge Huang

Received: 30 January 2023

Revised: 21 February 2023

Accepted: 23 February 2023

Published: 24 February 2023



Copyright: © 2023 by the authors. Licensee MDPI, Basel, Switzerland. This article is an open access article distributed under the terms and conditions of the Creative Commons Attribution (CC BY) license (<https://creativecommons.org/licenses/by/4.0/>).

1. Introduction

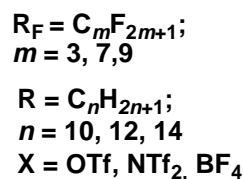
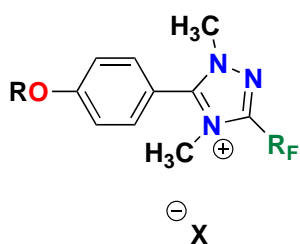
Ionic liquid crystals (ILCs) are organic, low-melting salts that give rise to liquid crystalline mesophases via self-assembly. Among the organic materials, thermotropic ILCs are considered appealing for their peculiar combination of low volatility, good solvent capability and their good ionic conductivity of ionic liquids (ILs) with the anisotropy of liquid crystals (LCs) that is typical for intrinsically ordered media [1,2]. These combined properties allow ILCs to be exploited in a variety of fields, such as acting as electrolytes for batteries, [3] in dye-sensitized solar cells, [4] in sensors, [5,6] and as water desalination membranes, [7] to cite a few. Aside from the widely explored cationic cores such as imidazolium and pyridinium, [8–10] other heterocyclic core ionic structures, such as oxadiazoles and triazoles, which have been mainly investigated for their biological activity, [11–14] are interesting for their predictable tuning of mesophase behavior [1,15] when segregations between polar charged regions and non-polar aliphatic chains are expected to drive self-assembly. Moreover, the presence of fluorocarbon chains would additionally stress self-organisation [9,16,17] and allow for the formation of ordered, smectic lamellar phases [18–21] with the appealing property of gas sorption [22].

In this context, we recently studied a set of 1,2,4-triazolium salts with a variable fluoroalkyl chain length (3, 7, 9), a variable alkyl chain length (10, 12, 14), and different anions that showed predominantly smectic A (SmA) phases [23,24]. Their liquid crystalline behaviour was dependent on the counterion and on the length of the perfluoroalkyl chain linked to the triazolium core of the salts [23,24].

On the grounds of these studies and being willing to modify the shape of the mesogen, we addressed our study to a new class of di-alkyloxy-phenyl-1,2,4 triazolium salts bearing a perfluoroalkyl chain of seven carbon atoms.

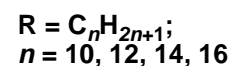
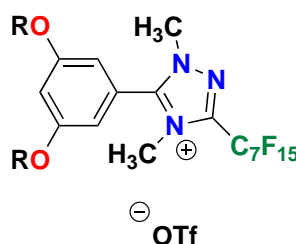
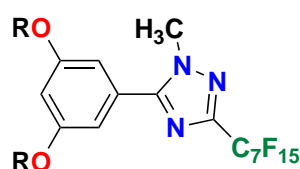
In Scheme 1, this new family of salts, which differs in the length of the alkyl chains, are summarized and compared to the previous work [23], in which the cation bore one alkoxy chain.

Previous work



Alkoxy-Phenyl-Triazolium salts: [Ph-Tri-m,n][X]

This work



Neutral precursors: Ph-Tri-(n)₂

Dialkoxy-Phenyl-Triazolium salts: [Ph-Tri-(n)₂][OTf]

Scheme 1. Structures of the 4-alkoxy-phenyl-1,2,4 triazolium salts previously studied in [23], 3,5-dialkoxy-phenyl-1,2,4 triazoles, and the corresponding trifluoromethanesulfonate salts studied in this work.

The synthesis, structure, and mesogenic properties of these trifluoromethanesulfonate triazolium salts are discussed as a function of the tuned, structural, variable length of the alkoxy chains on the phenyl ring ($n = 10, 12, 14$ or 16) and in comparison to the homologous set with one alkoxy chain reported in [23,24]. Differential scanning calorimetry (DSC), in combination with polarizing optical microscopy (POM), was exploited in order to investigate the thermotropic properties of this set of salts.

2. Materials and Methods

2.1. General

2.1.1. Materials

3,5-dimethoxybenzotrile, sodium hydroxide, hydroxylamine hydrochloride, methylhydrazine, boron tribromide, pentadecafluorooctanoyl chloride, potassium carbonate, 1-iodododecane, 1-iodotetradecane, 1-bromotetradecane, 1-bromohexadecane, methyl trifluoromethanesulfonate, ethyl acetate, petroleum ether, *N,N*-dimethylformamide, toluene, chloroform, ethanol (96%), acetonitrile, and pyridine were purchased from a commercial source and used as received.

2.1.2. Methods

¹H-NMR spectra were recorded on Bruker 300 MHz and 400 MHz spectrometers. ¹³C-NMR and ¹⁹F-NMR spectra were recorded on a Bruker 400 MHz spectrometer. The residual solvent peak was used as reference.

Reversed-phase HPLC/ESI/Q-TOF HRMS experiments were performed using mixtures of water and acetonitrile of HPLC/MS grade as eluents with the addition of 0.1% (*v/v*) of formic acid. The HPLC system was an Agilent 1260 Infinity. A reversed-phase C18 column (Luna Omega 5 μm Polar C18 150 × 2.1 mm) with a Phenomenex C18 security guard column (4 mm × 3 mm) was used. The flow rate was 1 mL/min, and the column

temperature was set to 40 °C. The eluent was varied, and its composition was changed with a linear gradient. Initially, for 10 min, the linear gradient passed from 95% to 5% water; for a further 10 min, the gradient was inverted and passed from 5% to 95% water and, for the last 5 min, turned to a gradient of 95% to 5% water. The volume injected was 10 µL. MS TIC was used to monitor the eluate. Mass spectra were registered on an Agilent 6540 UHD accurate-mass Q-TOF spectrometer equipped with a Dual AJS ESI source working in positive mode. N₂ was used as a desolvation gas at 300 °C and a flow rate of 9 L/min. The nebulizer was set to 45 psi. The Sheath gas temperature was set at 350 °C and a flow of 12 L/min. A potential of 3.5 kV was used on the capillary for positive ion mode. The fragmentor was set to 110 V. MS spectra were recorded in the 150–2000 *m/z* range.

A polarized optical microscopy (POM) analysis of the salts was performed on a Zeiss Axio imager.A2m microscope (Carl Zeiss, Göttingen, Germany) equipped with a Linkham hot-stage LTS420E with a Linkpad T95-LTS processor to control the temperature. The samples were placed between a glass slide and a cover slit and were heated and cooled at a rate of 5 °C min⁻¹. An Axiocam ICC1 digital camera mounted atop the microscope was used to collect photomicrographs. Images were recorded at magnifications of 5×, 10×, or 20× and in cross-polarized light.

Differential scanning calorimetry (DSC) measurements were carried out with a TA Instruments mod. 2920 Differential Scanning Calorimeter (TA Instrument Inc., New Castle, DE, USA) equipped with a TA Instruments Refrigerated Cooling System. Samples (~4 mg) were weighed in aluminium TA Tzero Hermetic Pans, which were subsequently sealed with aluminium lids. The analysis was performed with heating and cooling rates of 10 °C min⁻¹ under a N₂ atmosphere of 60 mL min⁻¹. Three heating and cooling ramps were carried out in a temperature range between –20 °C and 120 °C.

2.2. Synthesis of (Z)-N'-Hydroxy-3,5-Methoxybenzimidamide (2)

The synthesis of (Z)-N'-Hydroxy-3,5-methoxybenzimidamide (2) was carried out by modifying a previously reported procedure. The product obtained was in agreement with the one previously reported [25].

3,5-Dimethoxybenzotrile (1) (5 g; 30.6 mmol) was dissolved in EtOH (70 mL). A separate solution of NaOH (2.5 g; 2.0 mol eq.) was prepared in the minimal amount of water and hydroxylamine hydrochloride. NH₂OH·HCl, (4.31 g; 2.0 mol eq.) was added. The solutions were mixed and refluxed for 6 h; the reaction was monitored by TLC (petroleum ether and ethyl acetate 5:1). The reaction mixture was removed under a vacuum, then water (100 mL) was added to the residue and the precipitate was filtered and washed with cold water.

(Z)-N'-Hydroxy-3,5-methoxybenzimidamide (2): colourless solid. Yield = 94%. ¹H NMR (400 MHz, DMSO-d₆) δ, ppm: 3.80 (s, 6H), 5.87 (s, 2H), 6.55 (t, J = 2.2 Hz, 1H), 6.90 (d, J = 2.4 Hz, 2H), 9.7 (s, 1H). IR: ν (cm⁻¹) = 3452.3, 3354.0, 1679.9, 1598.9.

2.3. Synthesis of 1,2,4-Oxadiazole (3)

The 1,2,4-oxadiazole (3) was prepared as previously reported, reacting N'-Hydroxy-3,5-dimethoxybenzimidamide (2) with pentadecafluorooctanoyl chloride to obtain compound 3 [26]. Then, N'-Hydroxy-3,5-methoxybenzimidamide (2) (5.5 g, 28 mmol) was dissolved in toluene (75 mL). Pyridine (2.8 mL, 1.2 eq.) and pentadecafluorooctanoyl chloride (8.3 mL, 33.6 mmol) were then added to previous solution. The reaction mixture was refluxed for 6 h, and the reaction was monitored by TLC (petroleum ether and ethyl acetate 20:1). Subsequently, the mixture was evaporated, water (100 mL) was added, and the pH was adjusted with a NaHCO₃ solution. The organic compound was extracted with ethyl acetate (3 × 40 mL), and the organic phase was dried with Na₂SO₄. Compound 3 was isolated by chromatography, using petroleum ether/ethyl acetate 10:1 as eluents.

3-(3,5-di-methoxyphenyl)-5-(perfluoroheptyl)-1,2,4-oxadiazole (3): colourless solid. Yield = 34%. ¹H NMR (400 MHz, CDCl₃) δ, ppm: 3.84 (s, 6H), 6.72 (t, J = 4 Hz, 1H), 7.19

(d, $J = 4$ Hz, 2H). ESI-MS analysis for $[C_{17}H_9F_{15}N_2O_3]^+$: Calc.: 574.0403 g mol⁻¹, exp.: 574.0606 g mol⁻¹.

2.4. Synthesis of Compound (4)

The ANRORC (Addition of a Nucleophile with Ring Opening and Ring Closure) rearrangement of compound **3** into compound **4** was performed. This last product was finally demethylated to obtain corresponding triazole **5** [27–29].

First, 3-(3,5-di-methoxyphenyl)-5-(perfluoroheptyl)-1,2,4-oxadiazole (**3**) (0.6 g, 1.04 mmol) was dissolved separately in DMF (3 mL), and methylhydrazine (10 mmol, 0.55 mL) was added to the solution. The reaction mixture was stirred and heated at 150 °C for 2 h in a sealed tube. After cooling, water was added (100 mL), and the pH was brought to neutral using dilute HCl. Following extraction with diethyl ether (3 × 40 mL), the organic phase was dried with Na₂SO₄. The compound (**4**) was then isolated and purified by chromatography (using petroleum ether/ethyl acetate 5:1).

5-(3,5-di-methoxyphenyl)-1-methyl-3-(perfluoroheptyl)-1,2,4-triazole (4): colourless solid. Yields = 80%. ¹H NMR (400 MHz, CD₃CN) δ , ppm: 3.65 (s, 6H), 4.09 (s, 3H), 6.67 (t, $J = 3$ Hz, 1H), 6.86 (d, $J = 3$ Hz, 2H). ESI-MS analysis for $[C_{18}H_{12}F_{15}N_3O_2 + H^+]$: Calc.: 588.2570 g mol⁻¹, exp.: 588.0869 g mol⁻¹.

2.5. Synthesis of Compound (5)

Boron tribromide (3.5 mL) was added by cannula under an inert atmosphere to a solution of triazole **4** (0.9 g, 1.5 mmol) in dried toluene (50 mL). The mixture was refluxed for 3 h, and the reaction was monitored by TLC (petroleum ether and ethyl acetate 5:1). Water was then added (30 mL) to the mixture, which was heated for 1 additional hour. After cooling, the mixture was evaporated, further water was added, and the organic compound was extracted with ethyl acetate (3 × 40 mL). The organic phase was dried with Na₂SO₄, and compound **5** was isolated by chromatography, using petroleum ether/ethyl acetate 5:1 and 2:1 as eluents.

5-(1-methyl-3-(perfluoroheptyl)1H-1,2,4-triazol-5-yl)benzene-1,3-diol (5): colourless solid. Yields = 93%. ¹H NMR (400 MHz, DMSO-*d*₆) δ , ppm: 4.05 (s, 3H), 6.42 (t, $J = 3$ Hz, 1H), 6.65 (d, $J = 3$ Hz, 2H), 9.72 (s, 2H). ESI-MS analysis for $[C_{16}H_8F_{15}N_3O_2 + H^+]$: Calc.: 560.0450 g mol⁻¹, exp.: 560.0451 g mol⁻¹.

2.6. Synthesis of Triazole Precursors

Triazole **5** (0.40 g, 0.72 mmol) was dissolved in acetonitrile (5 mL) in a sealed tube. K₂CO₃ (6 eq., 0.6 g) was then added, and the mixture was stirred at 80 °C for 2 h. Afterwards, 3 eq. (2.16 mmol) of the corresponding iodo- or bromo-alkane (1-iodododecane, 1-iodotetradecane, 1-bromotetradecane, 1-bromohexadecane) were added to the mixture. The obtained mixture was heated at 80 °C for 1.5 to 6 h in dependence of iodo- or bromo-alkane. The reactions were monitored by TLC (petroleum ether and ethyl acetate 5:1). After cooling, the mixture was evaporated, water was added (50 mL), and the organic compounds were extracted with ethyl acetate (3 × 30 mL). The organic phase was dried with Na₂SO₄, and the neutral triazoles were isolated by chromatography, using petroleum ether/ethyl acetate 20:1 and 5:1 as eluents.

5-(3,5-bis(decyloxy)phenyl)-1-methyl-3-(perfluoroheptyl)-1H-1,2,4-triazole-Ph-Tri-(10)₂: white solid. Yield = 78% ¹H NMR (400 MHz, CDCl₃) δ , ppm: 0.88 (t, $J = 8$ Hz, 6H), 1.28 (m, 24H), 1.45 (q, $J = 8$ Hz, 4H), 1.79 (q, $J = 4$ Hz, 4H), 3.98 (t, $J = 8$ Hz, 4H), 4.07 (s, 3H), 6.60 (t, 1H), 6.76 (d, 2H). ESI-MS analysis for $[C_{36}H_{48}F_{15}N_3O_2 + H^+]$: Calc.: 840.3580 g mol⁻¹, exp.: 840.3617 g mol⁻¹.

5-(3,5-bis(dodecyloxy)phenyl)-1-methyl-3-(perfluoroheptyl)-1H-1,2,4-triazole-Ph-Tri-(12)₂: white solid. Yield = 75% ¹H NMR (300 MHz, CDCl₃) δ , ppm: 0.88 (t, $J = 6$ Hz, 6H), 1.26 (m, 32H), 1.45 (m, 4H), 1.78 (m, 4H), 3.98 (t, $J = 6$ Hz, 4H), 4.07 (s, 3H), 6.59 (t, 1H), 6.76 (d, 2H). ESI-MS analysis for $[C_{40}H_{56}F_{15}N_3O_2 + H^+]$: Calc.: 896.4206 g mol⁻¹, exp.: 896.4234 g mol⁻¹.

5-(3,5-bis(tetradecyloxy)phenyl)-1-methyl-3-(perfluoroheptyl)-1H-1,2,4-triazole-Ph-Tri-(14)₂: white solid. Yield = 82% ¹H NMR (300 MHz, CDCl₃) δ, ppm: 0.87 (t, J = 6 Hz, 6H), 1.26 (m, 40H), 1.45 (m, 4H), 1.78 (m, 4H), 3.98 (t, J = 6 Hz, 4H), 4.07 (s, 3H), 6.59 (t, 1H), 6.76 (d, 2H). ESI-MS analysis for [C₄₄H₆₄F₁₅N₃O₂ + H⁺]: Calc.: 952.4832 g mol⁻¹, exp.: 952.4947 g mol⁻¹.

5-(3,5-bis(hexadecyloxy)phenyl)-1-methyl-3-(perfluoroheptyl)-1H-1,2,4-triazole-Ph-Tri-(16)₂: white solid. Yield = 82% ¹H NMR (300 MHz, CDCl₃) δ, ppm: 0.87 (t, J = 6 Hz, 6H), 1.25 (m, 48H), 1.45 (m, 4H), 1.78 (m, 4H), 3.98 (t, J = 6 Hz, 4H), 4.07 (s, 3H), 6.60 (t, 1H), 6.76 (d, 2H). ESI-MS analysis for [C₄₈H₇₂F₁₅N₃O₂ + H⁺]: Calc.: 1008.5458 g mol⁻¹, exp.: 1008.5497 g mol⁻¹.

2.7. Synthesis of Trifluoromethanesulfonate Triazolium Salts

To a solution of neutral triazole (0.25 g, 0.26 mmol) in toluene (10 mL), 0.4 mL (15 eq.) of CF₃SO₃CH₃ was added in a sealed tube. The mixture was stirred and heated at 110 °C for 24 h. The reaction mixture was dried under a vacuum, and the compounds [Ph-Tri-(n)₂][OTf] were isolated by chromatography, using petroleum ether/ethyl acetate 20:1 and 3:1 as eluents.

5-(3,5-bis(decyloxy)phenyl)-1,4-dimethyl-3-(perfluoroheptyl)-1H-1,2,4-triazol-4-ium trifluoromethanesulfonate [Ph-Tri-(10)₂][OTf]: white solid. Yield = 30% ¹H NMR (300 MHz, CD₃OD) δ, ppm: 0.93 (t, J = 6 Hz, 6H), 1.32 (m, 28H), 1.83 (m, 4H), 3.95 (s, 3H), 4.01 (t, J = 6 Hz, 4H), 4.13 (s, 3H), 6.91 (d, J = 3 Hz, 2H), 6.95 (d, 1H). ESI-MS analysis for [C₃₇H₅₁F₁₅N₃O₂⁺]: Calc.: 854.3736 g mol⁻¹, exp.: 854.3794 g mol⁻¹.

5-(3,5-bis(dodecyloxy)phenyl)-1,4-dimethyl-3-(perfluoroheptyl)-1H-1,2,4-triazol-4-ium trifluoromethanesulfonate [Ph-Tri-(12)₂][OTf]: white solid. Yield = 32% ¹H NMR (300 MHz, CD₃CN) δ, ppm: 0.88 (t, J = 6 Hz, 6H), 1.28 (m, 32H), 1.45 (m, 4H), 1.77 (m, 4H), 3.81 (s, 3H), 4.01 (m, 4H), 4.04 (m, 3H), 6.73 (m, 2H), 6.86 (s, 1H). ESI-MS analysis for [C₄₁H₅₉F₁₅N₃O₂⁺]: Calc.: 910.4368 g mol⁻¹, exp.: 910.4394 g mol⁻¹.

5-(3,5-bis(tetradecyloxy)phenyl)-1,4-dimethyl-3-(perfluoroheptyl)-1H-1,2,4-triazol-4-ium trifluoromethanesulfonate [Ph-Tri-(14)₂][OTf]: white solid. Yield = 41% ¹H NMR (300 MHz, CDCl₃) δ, ppm: 0.87 (t, J = 6 Hz, 6H), 1.25 (m, 40H), 1.44 (m, 4H), 1.78 (m, 4H), 3.92 (s, 3H), 4.02 (t, J = 6 Hz, 4H), 4.11 (s, 3H), 6.77 (m, 1H), 6.95 (d, 2H). ESI-MS analysis for [C₄₅H₆₇F₁₅N₃O₂⁺]: Calc.: 966.4950 g mol⁻¹, exp.: 966.4989 g mol⁻¹.

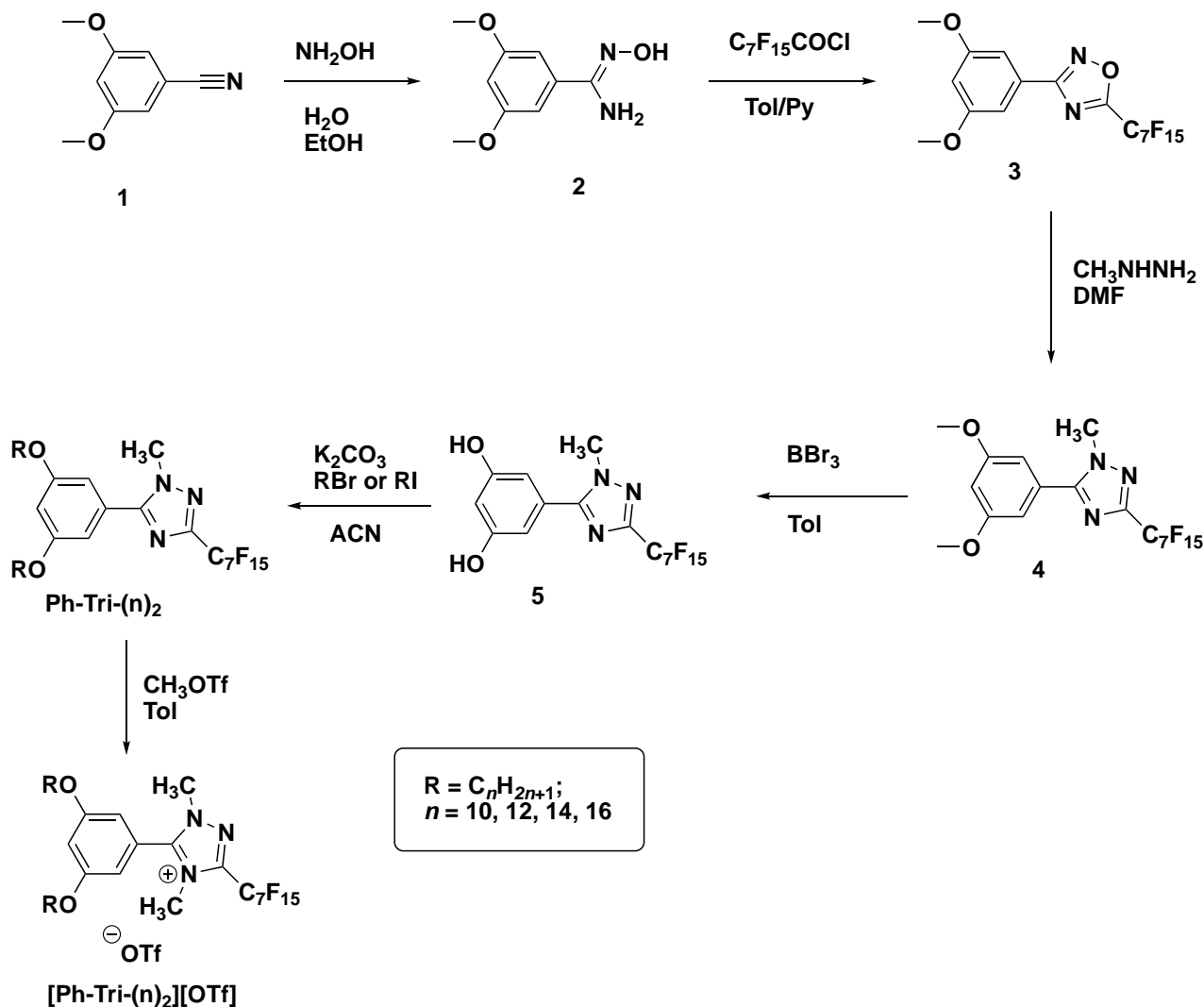
5-(3,5-bis(hexadecyloxy)phenyl)-1,4-dimethyl-3-(perfluoroheptyl)-1H-1,2,4-triazol-4-ium trifluoromethanesulfonate [Ph-Tri-(16)₂][OTf]: white solid. Yield = 30% ¹H NMR (300 MHz, CDCl₃) δ, ppm: 0.87 (t, J = 6 Hz, 6H), 1.25 (m, 48H), 1.44 (m, 4H), 1.78 (m, 4H), 3.92 (s, 3H), 4.01 (t, J = 6 Hz, 4H), 4.10 (s, 3H), 6.77 (s, 1H), 6.94 (s, 2H). ESI-MS analysis for [C₄₉H₇₅F₁₅N₃O₂⁺]: Calc.: 1022.5614 g mol⁻¹, exp.: 1022.5787 g mol⁻¹.

3. Results and Discussion

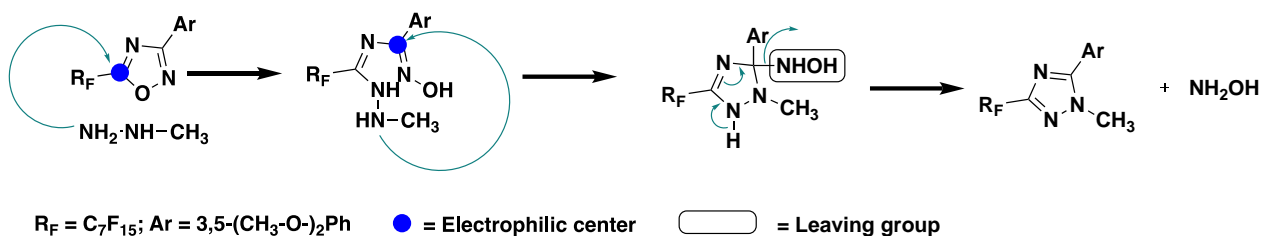
3.1. Synthesis of ILCs

The synthesis of the ILCs followed a previously reported synthetic route in which 1,2,4-oxadiazole (3) was obtained from the reaction between amidoxime (2), previously formed, and the selected perfluoroacyl chloride (Scheme 2). The obtained oxadiazole precursor then underwent a nucleophilic attack by methylhydrazine and, through the ANRORC rearrangements (Addition of a Nucleophile, Ring-Opening, Ring-Closure), the 1,2,4-triazole intermediate (4) was formed [27–29]. The proposed mechanism of this rearrangement comprised an initial attack of the nucleophile at the C(5) position of the 1,2,4-oxadiazole, involving the less-hindered NH₂ end of methylhydrazine. The nucleophile attack caused the ring opening. This was followed by a subsequent intramolecular nucleophilic attack at the (C3) position, leading to triazole formation after coming out of the leaving group (Scheme 3) [30]. Thus obtained, the 1,2,4-triazole (4) underwent demethylation with BBr₃ to form intermediate (5), which was then subjected to alkylation with long chain alkyl bromides or iodides, giving rise to the corresponding dialkyloxy-phenyl-1,2,4-triazoles, **Ph-Tri-(n)₂**, in a good yield and with a high purity. Finally, the obtained

triazoles were alkylated with methyl trifluoromethanesulfonate in toluene giving rise to trifluoromethanesulfonate 1,2,4-triazolium salts [**Ph-Tri-(n)₂**][OTf] (Scheme 2). According to previous studies, the methylation for 3,5-disubstituted-1,2,4-triazoles occurred at a sterically less-hindered and the more nucleophilic N(4) site [23].



Scheme 2. Synthetic route through which 3,5 dialkoxy-phenyl-1,2,4 triazolium trifluoromethanesulfonate was obtained.



Scheme 3. Proposed mechanism for the ANRORC rearrangements [30].

Trifluoromethanesulfonate 1,2,4-triazolium salts showed the characteristic triflate signal at -79.9 ppm in the ^{19}F NMR spectrum. All F signals can be distinguished contrary to what observed for the ^{19}F NMR spectrum of the corresponding neutral precursor, **Ph-Tri-(n)₂**, in which two fluorine peaks were superimposed at -122.5 (Figures S6 and S7 of Supplementary Materials).

3.2. Thermal Analysis

The liquid crystalline properties of neutral precursors and triazolium salts have been studied by DSC and POM analyses. A DSC analysis of each sample was performed using a heating and cooling temperature ramp of $10\text{ }^{\circ}\text{C min}^{-1}$. It was reproducible for three cycles.

Neutral triazoles did not show any liquid crystalline behaviour as, upon cooling, the DSC trace showed only one exothermic peak. In general, an increase in the melting temperature (T_m) of the compounds can be observed with the increase in the length of the alkyloxy chains (Table 1).

Table 1. Melting temperatures (T_m) and enthalpies (ΔH) of neutral triazole compounds obtained from the DSC traces upon heating.

Neutral Triazole	T_m ($^{\circ}\text{C}$) ^a	ΔH (kJ mol^{-1})
Ph-Tri-(10) ₂	22.7	36.8
Ph-Tri-(12) ₂	40.6	57.5
Ph-Tri-(14) ₂	53.2	76.9
Ph-Tri-(16) ₂	59.8	78.9

^a Transitions refer to the second heating cycles. Temperatures indicate the onset of each peak.

The alkylation of the neutral triazoles and the formation of the corresponding salts awarded the liquid crystalline behaviour to the compounds. In all cases, at least two distinct transitions can be observed from the cooling calorimetric traces (Figure 1). The first transition of the cooling cycle after heating corresponds to the clearing point (T_c) from the isotropic solution to the mesophase and the following transition as the melting point (T_m). In one case, two distinct transitions can be observed before the formation of the crystals.

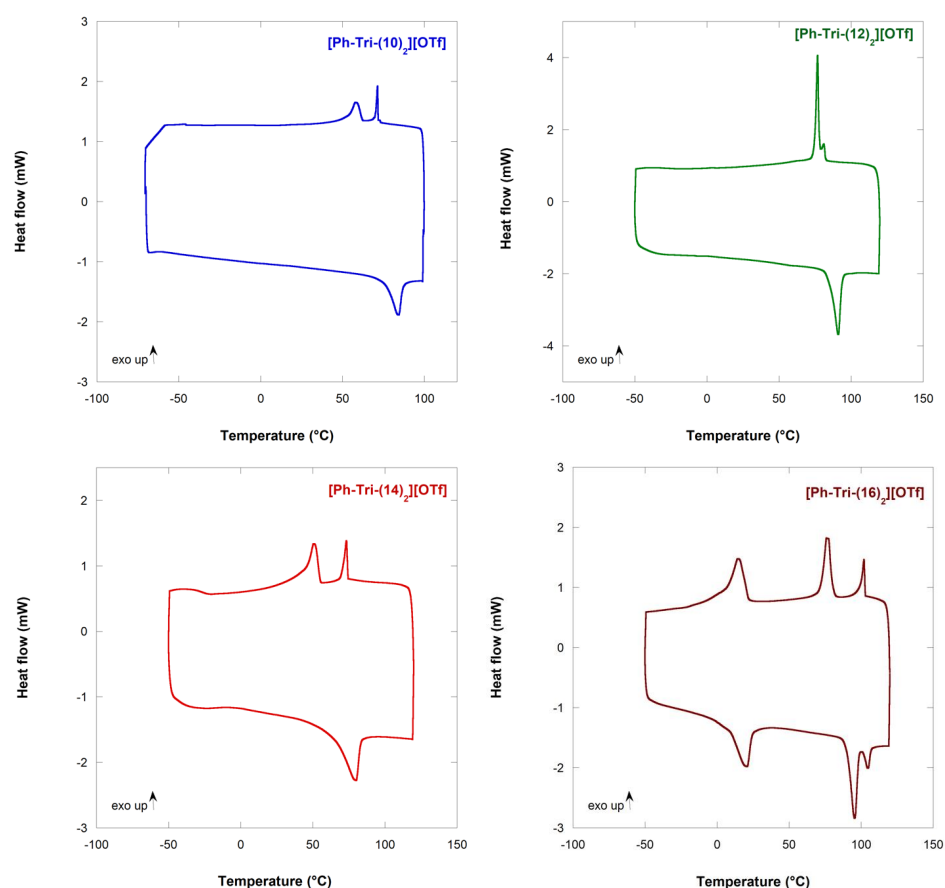


Figure 1. DSC traces of ILCs showing the second cooling and heating cycles. Exothermic peaks point upward.

The increase in the alkyloxy chain length on the phenyl ring of the triazolium salts caused an increase in T_c , passing from 71.8 °C to 102.7 °C for [Ph-Tri-(10)₂][OTf] and [Ph-Tri-(16)₂][OTf], respectively (Table 2). However, [Ph-Tri-(14)₂][OTf] showed a deviation from the above trend as a decrease in T_c value was recorded for this salt. The observed increase in clearing points with an increasing chain length are in agreement with what was previously reported as longer hydrocarbon chains increase the van der Waals forces among the alkoxy moieties, inducing micro-segregation between the hydrophobic alkyl chains and charged ionic regions [10].

Table 2. Transition temperatures (T), enthalpies (ΔH) and phase transition of the salts obtained from DSC traces upon cooling.

ILCs	T (°C) ^a	ΔH (kJ mol ⁻¹)	Transition ^b
[Ph-Tri-(10) ₂][OTf]	71.8	2.6	Iso-LC (Col)
	62.1	6.7	LC (Col)-Cr
[Ph-Tri-(12) ₂][OTf]	81.3	0.9	Iso-LC (Col)
	76.6	10.6	LC (Col)-Cr
[Ph-Tri-(14) ₂][OTf]	74.3	2.6	Iso-LC (Col)
	54.6	7.3	LC (Col)-Cr'
[Ph-Tri-(16) ₂][OTf]	102.7	3.1	Iso-LC (Col)
	80.1	12.6	LC (Col)-LC (Col _h)
	21.9	10.5	LC (Col _h)-Cr

^a Transitions refer to the second cooling cycles. Temperatures indicate the onset of each peak. ^b Abbreviations: Iso— isotropic phase; LC—liquid crystalline phase; Col—columnar, Col_h—columnar hexagonal; and Cr—crystalline solid state.

Interestingly, passing from 14 hydrocarbon chains to longer alkyloxy chains (16), more than one transition can be recognized and, moreover, the transitions to mesophases are observable both in cooling and heating ramps.

Comparing the data from Table 2 with the literature, the transition temperatures and the corresponding enthalpies could be suggestive of phase transitions [2,31].

From the enthalpy values, it can be assumed that, in all cases, the first exothermic peak can be ascribed to a transition from the isotropic liquid into the liquid crystalline phase (Iso-LC). The second transition probably refers to the transition from the liquid crystalline phase into the crystalline solid-state form (LC-Cr) when only two exothermic peaks appear in DSC, i.e., [Ph-Tri-(10)₂][OTf], [Ph-Tri-(12)₂][OTf] and [Ph-Tri-(14)₂][OTf]. On the other hand, for [Ph-Tri-(16)₂][OTf], a different scenario is observed: three exothermic peaks appear in the DSC trace. A transition between two different liquid crystalline phases can be hypothesized before the formation of a crystalline phase, even if the enthalpy value associated to a possible LC-LC transition seems high. The combination of DSC data and the POM analysis can shed light on the transitions occurring during the heating and cooling cycles of the salts.

The liquid crystalline behaviour of the salts was confirmed by the POM analysis. The first transitions observed during the POM analysis confirmed the transition analysed by DSC; each sample was heated and cooled at 5 °C min⁻¹. For each salt, a change from the dark isotropic liquid phase into a birefringent phase was observed upon cooling.

The mesophases after the full transition are shown in Figures 2 and 3, demonstrating typical liquid crystalline textures. The hypotheses based on DSC data that the first transition refers to the Iso-LC transition and the second to a LC-Cr transition were supported by the POM analysis. However, transitions between two different liquid crystalline forms (LC-LC) or from a crystalline solid-state to another (Cr''-Cr') transition could be hardly identified by POM, even if some information could also be extrapolated. The compounds are classified as monotropic ionic liquid crystals as two distinct transitions were observed only upon cooling. However, the further increase in the alkyloxy chain on the phenyl ring brought

enantiotropic ionic liquid crystals for $[\text{Ph-Tri-(16)}_2][\text{OTf}]$ as the mesophases are reversibly formed during heating and cooling cycles.

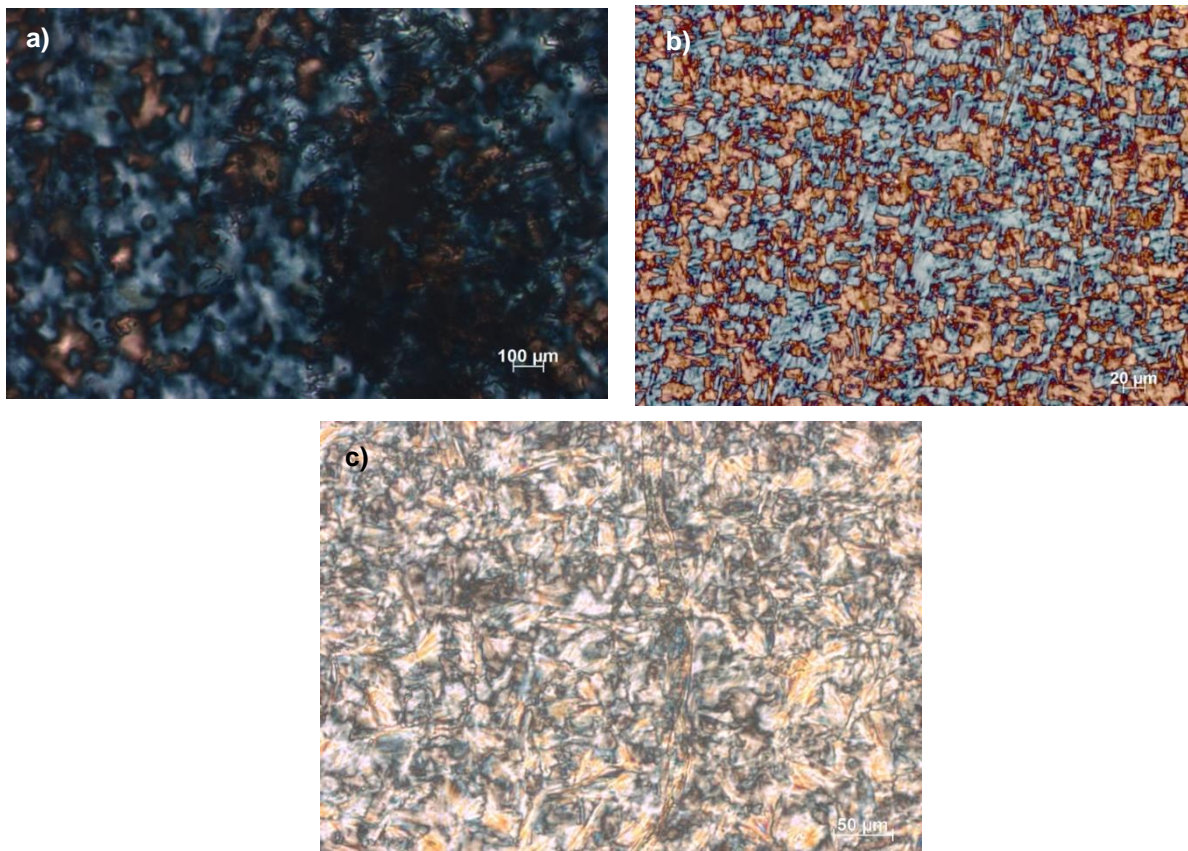


Figure 2. Optical textures of: (a) $[\text{Ph-Tri-(10)}_2][\text{OTf}]$ at 69 °C, (b) $[\text{Ph-Tri-(12)}_2][\text{OTf}]$ at 77 °C and (c) $[\text{Ph-Tri-(14)}_2][\text{OTf}]$ at 57 °C, obtained by polarized optical microscopy analysis under crossed polarizers showing the mesophase after the first transition from the isotropic liquid to the liquid crystalline phase upon cooling at 5 °C min⁻¹.

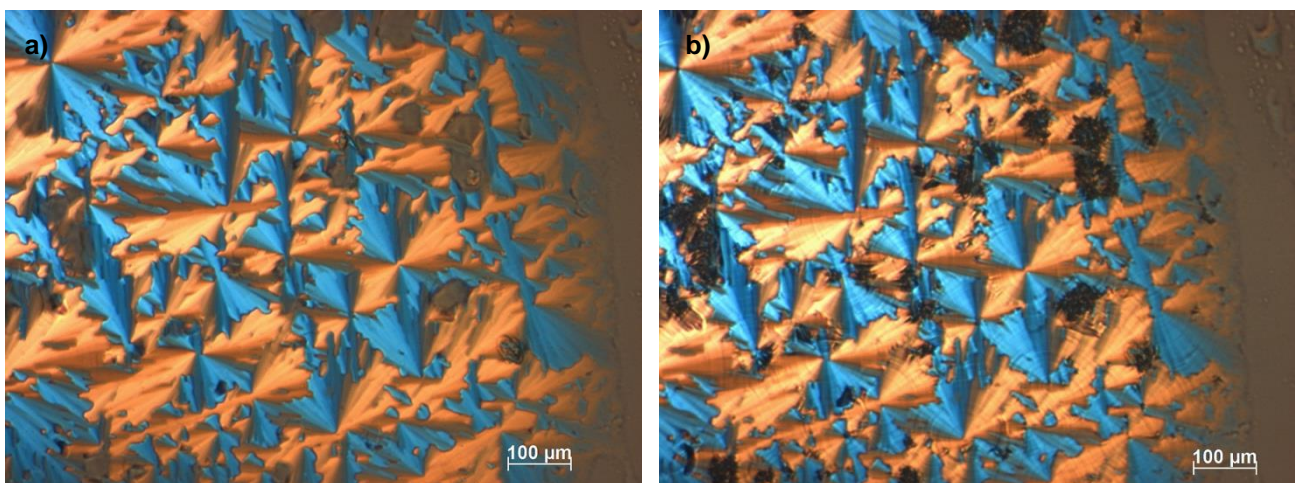


Figure 3. Optical textures of $[\text{Ph-Tri-(16)}_2][\text{OTf}]$ (a) at 92 °C and (b) 67 °C. Images observed by polarized optical microscopy analysis under crossed polarizers showing (a) the mesophase after the first transition from the isotropic liquid to the liquid crystalline phase and (b) the LC-LC transition upon cooling with 5 °C min⁻¹.

Comparing the optical textures of these salts with the ones previously reported and considering the cation shape, columnar mesophases are envisageable in all cases. These are the most commonly observed for ionic liquid crystals in addition to smectic A mesophases for rod-like cations [2,32]. All ILCs showed the typical morphology of mesophases at the POM analysis at the same transition temperatures previously observed by the DSC analysis.

For ILCs with dialkyloxy chains comprised of 10 to 14 carbon atoms, the microscopy analysis showed the mesophase after the first transition from the isotropic liquid to the liquid crystalline phase. In Figure 2, the typical morphological structure of the liquid crystalline phase that can be identified as a columnar mesophase can be observed, different from what was previously observed for a phenyl ring bearing a mono alkyloxy chain in which a smectic A (SmA) mesophase was recognized [23]. The presence of two alkyloxy chains on a phenyl ring likely awarded a trigonal geometry to the molecule instead of the banana-shaped structures observed for mono alkyloxy salts. This trigonal geometry could favour the supramolecular stacking and the formation of columnar mesophases in contrast to the SmA mesophases previously observed for bent cations [23].

Additionally, the three transitions observed at DSC for [Ph-Tri-(16)₂][OTf] were confirmed by the POM analysis. Figure 3a shows the liquid crystalline columnar mesophase obtained after the first transition from isotropic liquid solution, while Figure 3b can be indicative of a more structured liquid crystalline mesophase that can be recognized as a liquid crystalline columnar hexagonal mesophase. This is different for the appearance of striations across the fans, which is indicative of additional order growing. The presence of an LC phase columnar (Col) and hexagonal columnar (Col_h) is in agreement with what was previously observed for ILCs with a rigid core linked to long alkyl chains [33,34].

The comparison of ILC mesophase ranges sheds light on the presence of a wider mesophase range increasing the length of dialkyloxy chains on the phenyl unit of ILCs. This is in agreement with what was previously observed for the corresponding monoalkyloxy triflate ILCs (Figure 4) [23]. The temperature range in which the presence of mesophases can be observed ranges from 10 °C for [Ph-Tri-(10)₂][OTf] to 20 °C for [Ph-Tri-(14)₂][OTf] and up to 80 °C for [Ph-Tri-(16)₂][OTf]. The only exception to this trend is the shortest mesophase range of 5 °C, which was observed for [Ph-Tri-(12)₂][OTf]. On the other hand, the widest mesophase temperature range, from 102 to 22 °C, was displayed by [Ph-Tri-(16)₂][OTf], which was the only one to demonstrate two different forms of liquid crystalline mesophases, LC (Col)-LC (Col_h). The mesophase range observed for dialkyloxy triflate ILCs is narrower than the range of the corresponding monoalkyloxy ILCs. Indeed, columnar mesophases can be recognized instead of SmA phases.

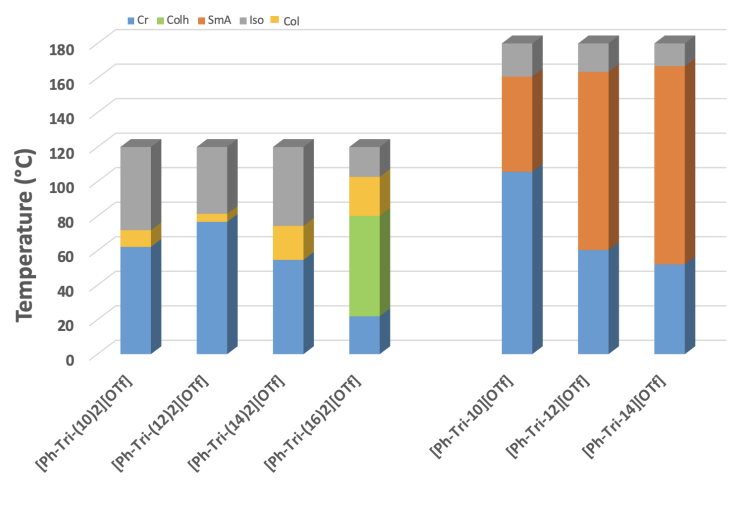


Figure 4. Plot of transition temperatures of LCs reported in this work and in previously reported data [23]. Abbreviations: Iso— isotropic phase; LC—iquid crystalline phase; Col—columnar, Col_h—columnar hexagonal, SmA—smectic A phase, Cr—crystalline solid state.

4. Conclusions

A new series of ILCs have been synthesized and their ionic liquid crystalline behaviour has been investigated by combining DSC and POM analyses.

The salts gained a liquid crystalline behaviour when compared to the neutral triazoles. Different from what was previously observed for mono alkyloxy phenyl triazolium salts, all ILCs showed the presence of a liquid crystalline phase that can be identified as columnar instead of smectic A. Due to the different shape of cations, a different kind of aggregation is envisageable. A wider range of mesophase can be observed by increasing the length of the dialkyloxy chain linked to the phenyl ring. With a higher length of the alkoxy chains, the appearance of more than one liquid crystalline form can be observed. In particular, increasing the dialkyloxy chains to 16 brings to a further transition from two different mesophases defined as Col and Col_h.

The different functionalization of the phenyl ring linked to the triazolium cation expands the family of triazolium ILCs and opens up the formation of new ILCs with different shapes that show several mesophases. The trigonal structure formed by the dialkyloxy triazolium salts shows columnar mesophases instead of the SmA phases previously observed for the banana-shaped structure of monoalkyloxy triazolium salts.

Supplementary Materials: The following supporting information can be downloaded at: <https://www.mdpi.com/article/10.3390/app13052947/s1>, Figures S1–S5. Representative ¹³C NMR spectra of new compounds. Figures S6 and S7. Representative ¹⁹F NMR spectra of new compounds.

Author Contributions: Conceptualization, I.P.; Methodology, A.P.; Formal analysis, C.R. and I.F.; Investigation, A.P.P.; Writing—original draft, C.R.; Writing—review & editing, A.P.P., A.P. and I.P.; Visualization, S.B.; Supervision, I.P.; Funding acquisition, C.R. and I.P. All authors have read and agreed to the published version of the manuscript.

Funding: I.P. thanks the University of Palermo, FFR2022. C.R. thanks PNR, Next Generation EU, DM737/2021, CUP B79J21038330001 for funding.

Institutional Review Board Statement: Not applicable.

Informed Consent Statement: Not applicable.

Data Availability Statement: All new data are available in Supplementary Materials.

Acknowledgments: The authors are grateful to Alberto Spinella for precious help with the Fluorine NMR analyses.

Conflicts of Interest: The authors declare no conflict of interest.

References

1. Goossens, K.; Lava, K.; Bielawski, C.W.; Binnemans, K. Ionic liquid crystals: Versatile materials. *Chem. Rev.* **2016**, *116*, 4643–4807. [[CrossRef](#)]
2. Kapernaum, N.; Lange, A.; Ebert, M.; Grunwald, M.A.; Haegel, C.; Marino, S.; Zens, A.; Taubert, A.; Giesselmann, F.; Laschat, S. Current topics in ionic liquid crystals. *ChemPlusChem* **2022**, *87*, e202100397. [[CrossRef](#)]
3. Nagaraj, M.; Lehmann, A.; Prehm, M.; Tschierske, C.; Vij, J.K. Evidence of a polar cybotactic smectic A phase in a new fluorine substituted bent-core compound. *J. Mater. Chem.* **2011**, *21*, 17098–17103. [[CrossRef](#)]
4. Ruan, Q.; Yao, M.; Yuan, D.; Dong, H.; Liu, J.; Yuan, X.; Fang, W.; Zhao, G.; Zhang, H. Ionic liquid crystal electrolytes: Fundamental, applications and prospects. *Nano Energy* **2023**, *106*, 108087. [[CrossRef](#)]
5. Safavi, A.; Tohidi, M. Design and characterization of liquid crystal—Graphite composite electrodes. *J. Phys. Chem.* **2010**, *114*, 6132–6140. [[CrossRef](#)]
6. Shvedene, N.V.; Avramenko, O.A.; Baulin, V.E.; Tomilova, L.G.; Pletnev, I.V. Iodide-Selective Screen-Printed Electrodes Based on Low-Melting Ionic Solids and Metallated Phthalocyanine. *Electroanalysis* **2011**, *23*, 1067–1072. [[CrossRef](#)]
7. Henmi, M.; Nakatsuji, K.; Ichikawa, T.; Tomioka, H.; Sakamoto, T.; Yoshio, M.; Kato, T. Self-organized liquid-crystalline nanostructured membranes for water treatment: Selective permeation of ions. *Adv. Mater.* **2012**, *24*, 2238–2241. [[CrossRef](#)]
8. Axenov, K.V.; Laschat, S. Thermotropic ionic liquid crystals. *Materials* **2011**, *4*, 206–259. [[CrossRef](#)]
9. Pibiri, I.; Beneduci, A.; Carraro, M.; Causin, V.; Casella, G.; Corrente, G.A.; Chidichimo, G.; Pace, A.; Riccobono, A.; Saielli, G. Mesomorphic and electrooptical properties of viologens based on non-symmetric alkyl/polyfluoroalkyl functionalization and on an oxadiazolyl-extended bent core. *J. Mater. Chem.* **2019**, *7*, 7974–7983. [[CrossRef](#)]

10. Weber, M.S.; Schulze, M.; Lazzara, G.; Piccionello, A.P.; Pace, A.; Pibiri, I. Oxadiazolyl-Pyridinium as Cationic Scaffold for Fluorinated Ionic Liquid Crystals. *Appl. Sci.* **2021**, *11*, 10347. [[CrossRef](#)]
11. Abu-Hashem, A.A. Synthesis and antimicrobial activity of new 1,2,4-triazole, 1,3,4-oxadiazole, 1,3,4-thiadiazole, thiopyrane, thiazolidinone, and azepine derivatives. *J. Heterocycl. Chem.* **2021**, *58*, 74–92. [[CrossRef](#)]
12. Abu-Hashem, A.A.; Al-Hussain, S.A. Design, synthesis of new 1, 2, 4-triazole/1, 3, 4-thiadiazole with spiroindoline, imidazo [4, 5-b] quinoxaline and thieno [2, 3-d] pyrimidine from isatin derivatives as anticancer agents. *Molecules* **2022**, *27*, 835. [[CrossRef](#)]
13. Pibiri, I.; Buscemi, S. A recent portrait of bioactive triazoles. *Curr. Bioact. Compd.* **2010**, *6*, 208–242. [[CrossRef](#)]
14. Pibiri, I.; Lentini, L.; Tutone, M.; Melfi, R.; Pace, A.; Di Leonardo, A. Exploring the readthrough of nonsense mutations by non-acidic Ataluren analogues selected by ligand-based virtual screening. *Eur. J. Med. Chem.* **2016**, *122*, 429–435. [[CrossRef](#)]
15. Dingemans, T.J.; Murthy, N.S.; Samulski, E.T. Javelin-, hockey stick-, and boomerang-shaped liquid crystals. Structural variations on p-quinquephenyl. *J. Phys. Chem.* **2001**, *105*, 8845–8860. [[CrossRef](#)]
16. Hird, M. Fluorinated liquid crystals—properties and applications. *Chem. Soc. Rev.* **2007**, *36*, 2070–2095. [[CrossRef](#)]
17. Tschierske, C. *Liquid Crystals: Materials Design and Self-Assembly*; Tschierske, C., Ed.; Springer: Berlin/Heidelberg, Germany, 2012; pp. 1–108. [[CrossRef](#)]
18. Abate, A.; Petrozza, A.; Cavallo, G.; Lanzani, G.; Matteucci, F.; Bruce, D.W.; Houbenov, N.; Metrangolo, P.; Resnati, G. Anisotropic ionic conductivity in fluorinated ionic liquid crystals suitable for optoelectronic applications. *J. Mater. Chem.* **2013**, *1*, 6572–6578. [[CrossRef](#)]
19. Celso, F.L.; Pibiri, I.; Triolo, A.; Triolo, R.; Pace, A.; Buscemi, S.; Vivona, N. Study on the thermotropic properties of highly fluorinated 1, 2, 4-oxadiazolylpyridinium salts and their perspective applications as ionic liquid crystals. *J. Mater. Chem.* **2007**, *17*, 1201–1208. [[CrossRef](#)]
20. Zama, I.; Gorni, G.; Borzatta, V.; Cassani, M.C.; Crupi, C.; Di Marco, G. Fluorinated imidazolium salts having liquid crystal characteristics. *J. Mol. Liq.* **2016**, *223*, 749–753. [[CrossRef](#)]
21. Cavallo, G.; Abate, A.; Rosati, M.; Venuti, G.P.; Pilati, T.; Terraneo, G.; Resnati, G.; Metrangolo, P. Tuning of ionic liquid crystal properties by combining halogen bonding and fluorous effect. *ChemPlusChem* **2021**, *86*, 469–474. [[CrossRef](#)]
22. Almantariotis, D.; Gefflaut, T.; Pádua, A.A.H.; Coxam, J.Y.; Gomes, M.F.C. Effect of fluorination and size of the alkyl side-chain on the solubility of carbon dioxide in 1-alkyl-3-methylimidazolium bis (trifluoromethylsulfonyl) amide ionic liquids. *J. Phys. Chem.* **2010**, *114*, 3608–3617. [[CrossRef](#)] [[PubMed](#)]
23. Riccobono, A.; Lazzara, G.; Rogers, S.E.; Pibiri, I.; Pace, A.; Slattery, J.M.; Bruce, D.W. Synthesis and mesomorphism of related series of triphilic ionic liquid crystals based on 1, 2, 4-triazolium cations. *J. Mol. Liq.* **2021**, *321*, 114758. [[CrossRef](#)]
24. Riccobono, A.; Parker, R.R.; Whitwood, A.C.; Slattery, J.M.; Bruce, D.W.; Pibiri, I.; Pace, A. 1,2,4-Triazolium ions as flexible scaffolds for the construction of polyphilic ionic liquid crystals. *Chem. Commun.* **2018**, *54*, 9965–9968. [[CrossRef](#)] [[PubMed](#)]
25. Xu, L.-L.; Wu, Y.-F.; Wang, L.; Li, C.-C.; Li, L.; Di, B.; You, Q.-D.; Jiang, Z.-Y. Structure-activity and structure-property relationships of novel Nrf2 activators with a 1, 2, 4-oxadiazole core and their therapeutic effects on acetaminophen (APAP)-induced acute liver injury. *Eur. J. Med. Chem.* **2018**, *157*, 1376–1394. [[CrossRef](#)]
26. Kayukova, L.A. Synthesis of 1, 2, 4-oxadiazoles (a review). *Pharm. Chem. J.* **2005**, *39*, 539–547. [[CrossRef](#)]
27. Buscemi, S.; Pace, A.; Pibiri, I.; Vivona, N.; Lanza, C.Z.; Spinelli, D. Fluorinated Heterocyclic Compounds—The First Example of an Irreversible Ring-Degenerate Rearrangement on Five-Membered Heterocycles by Attack of an External Bidentate Nucleophile. *Eur. J. Org. Chem.* **2004**, *2004*, 974–980. [[CrossRef](#)]
28. Buscemi, S.; Pace, A.; Pibiri, I.; Vivona, N.; Spinelli, D. Fluorinated heterocyclic compounds. An expedient route to 5-perfluoroalkyl-1,2,4-triazoles via an unusual hydrazinolysis of 5-perfluoroalkyl-1,2,4-oxadiazoles: First examples of an ANRORC-like reaction in 1,2,4-oxadiazole derivatives. *J. Org. Chem.* **2003**, *68*, 605–608. [[CrossRef](#)]
29. Pibiri, I.; Pace, A.; Buscemi, S.; Vivona, N.; Malpezzi, L. Designing fluorous domains. Synthesis of a series of pyridinium salts bearing a perfluoroalkylated azole moiety. *Heterocycles* **2006**, *68*, 307–321.
30. Buscemi, S.; Pace, A.; Piccionello, A.P.; Pibiri, I.; Vivona, N.; Giorgi, G.; Mazzanti, A.; Spinelli, D. Five-to-six membered ring-rearrangements in the reaction of 5-perfluoroalkyl-1, 2, 4-oxadiazoles with hydrazine and methylhydrazine. *J. Org. Chem.* **2006**, *71*, 8106–8113. [[CrossRef](#)]
31. Singh, S.; Dunmur, D.A. *Liquid Crystals: Fundamentals*; World Scientific Publishing Co., Pte Ltd.: Singapore, 2022; pp. 58–59.
32. Saielli, G.; Margola, T.; Satoh, K. Tuning Coulombic interactions to stabilize nematic and smectic ionic liquid crystal phases in mixtures of charged soft ellipsoids and spheres. *Soft Matter* **2017**, *13*, 5204–5213. [[CrossRef](#)]
33. Artzner, F.; Veber, M.; Clerc, M.; Levelut, A.-M. Evidence of nematic, hexagonal and rectangular columnar phases in thermotropic ionic liquid crystals. *Liq. Cryst.* **1997**, *23*, 27–33. [[CrossRef](#)]
34. Takagi, K.; Yamauchi, K.; Kubota, S.; Nagano, S.; Hara, M.; Seki, T.; Murakami, K.; Ooyama, Y.; Ohshita, J.; Kondo, M.; et al. Fused π -conjugated imidazolium liquid crystals: Synthesis, self-organization, and fluorescence properties. *RSC Adv.* **2016**, *6*, 9152–9159. [[CrossRef](#)]

Disclaimer/Publisher’s Note: The statements, opinions and data contained in all publications are solely those of the individual author(s) and contributor(s) and not of MDPI and/or the editor(s). MDPI and/or the editor(s) disclaim responsibility for any injury to people or property resulting from any ideas, methods, instructions or products referred to in the content.